Available online at www.sciencedirect.com
ScienceDirect
Journal of the European Ceramic Society 29 (2009) 267–273
www.elsevier.com/locate/jeurceramsoc

Ballistic testing of transparent armour ceramics

E. Straßburger*

Fraunhofer-Institut für Kurzzeitdynamik, Ernst-Mach-Institut (EMI), Am Klingelberg 1, 79588 Efringen-Kirchen, Germany

Available online 9 June 2008

Abstract

The testing methodology for transparent armour is described. The focus of this paper is on the assessment of the protective strength of transparent ceramics being used in transparent armour systems. Not only the ballistic testing method but also experimental techniques which allow the visualization of damage and the projectile penetration are discussed. Visualization techniques are essential for understanding the mechanisms of interaction between projectile and target material. Ballistic tests results, high-speed photographs and flash-radiographs from experiments with transparent armour are presented.

Keywords: Transparent armour; Ballistic testing; Transparent ceramic; Ballistic limit; Dwell; Projectile erosion; Flash X-ray techniques

1. Introduction

Conventional transparent armour consists of glass laminates with polymer interlayers and backing. Comprehensive testing of glass–polycarbonate laminates with so-called armour piercing (AP) ammunitions, i.e. projectiles with a hard core material (steel, tungsten carbide or tungsten), has demonstrated that the core of the projectiles is hardly being eroded during penetration and does not break in most instances. Thus, targets of relatively high weight and thickness are needed in order to defeat AP threats with the traditional materials for transparent armour. A significant weight reduction can be achieved by means of a hard front layer of transparent ceramics. The concept of a hard transparent front layer of sapphire, which has the function to induce damage to the projectile core by erosion and fragmentation, was already introduced about three decades ago.[1] Progress in material technology over the last 30 years has also made available aluminium oxynitride (AlON),[2] magnesium aluminate spinel ($MgAl_2O_4$)[3] and sub-μm grain size polycrystalline α-Al_2O_3[4] as alternative ceramic materials which fulfil the requirements of transparency and hardness. The manufacturing technologies for these materials have reached a state-of-the-art, that the use of transparent ceramics for armour applications appears feasible in the medium-term.

The three main objectives of the study presented here were the following: first, the results of the tests should indicate the threshold ceramic thickness to effect erosion and fracture of the core of AP projectiles in order to achieve a significant weight saving compared to glass/polymer laminates. The second objective was to clarify, whether or not there is an optimum ceramic weight fraction in a ceramic/glass/polymer laminate with respect to the ballistic resistance. These two mentioned objectives refer to the optimization of transparent laminates with one type of ceramic front layer. However, the ballistic testing method should also be able to discriminate between the performances of different transparent ceramics. Therefore, the third objective was to clarify, which of the candidate front layer materials offers the highest protection.

2. Ballistic testing

In order to assess the ballistic resistance of transparent ceramics as part of a transparent armour system the following approach was chosen. The targets consisted of three main components: (1) a ceramic front layer of thickness between 1.3 mm and 8.3 mm, (2) a glass laminate consisting of one, two or three layers of soda-lime float glass and (3) a polycarbonate layer of 4 mm thickness. The three target components were clamped together by means of two steel frames. No glue was used in order to join the different target layers. The lateral dimensions of the ceramic tiles were in the range of ≈85–100 mm^2. The size of the ceramic tiles was chosen such, that on one hand the ballistic performance was not reduced compared to bigger tiles with the

* Tel.: +49 7626 9157 235: fax: +49 7626 9157 1235.
E-mail address: strassburger@emi.fraunhofer.de.

0955-2219/$ – see front matter © 2008 Elsevier Ltd. All rights reserved.
doi:10.1016/j.jeurceramsoc.2008.03.049

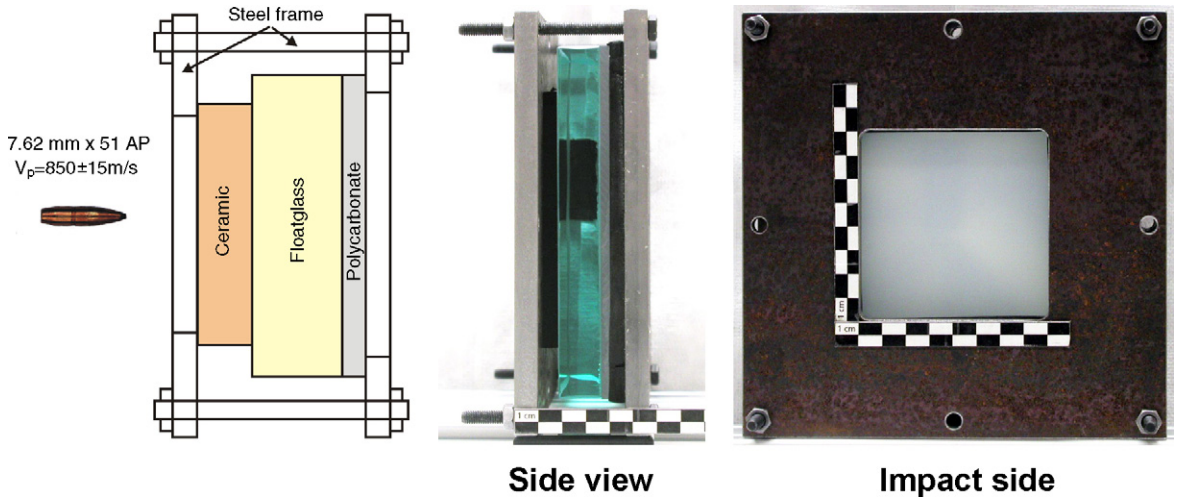

Fig. 1. Schematic and photographs of target assembly.

specific type of projectile used and on the other hand, the cost for the manufacture of the specimens was not higher than necessary. The glass and polycarbonate plates were of the dimensions 150 mm × 150 mm. Test series with stacks of glass plates of lateral dimensions 400 mm × 400 mm and 150 mm × 150 mm did not indicate a difference in the ballistic resistance. Thus, the smaller size was selected for the test series, where the performance against a single hit was assessed. Another test series with stacks of soda-lime float glass of total thickness 59 mm, which were assembled of either 4 layers or 10 layers of glass, revealed a lower ballistic resistance in the case of the higher number of layers. Since the objective of the study was the assessment of the performance of the ceramic front layer, the glass part of the targets was assembled from as little layers as necessary, in order to achieve the desired total thickness. The minimum thickness of a single layer was 8 mm. With the reduction of the numbers of glass layers also a reduction of the number of parameters was strived for. Fig. 1 shows a schematic of the target assembly and photographs of a typical target. Since the ceramics were not polished for the ballistic tests, it is not possible to look through the presented target.

The thickness range of the ceramic front layer was selected on the basis of two primary considerations. On one hand it is desirable to use not more ceramic material than necessary, due to the high costs of transparent ceramic compared to other materials used in conventional transparent armour. On the other hand there are the requirements for light transmission of transparent armour systems for application in vehicles. In order to prevent a reduced transmission with increasing thickness of the ceramic, the real in-line transmission has to be close to the theoretical limit of the material. At the time being transparent ceramics with real in-line transmission close to the theoretical limit are available.[5] However, at the time when this study was started it was assumed, that it would be easier to meet the transmission requirement for transparent armour systems with thin ceramic layers. Thus, configurations with thick ceramic layers and targets, consisting of a ceramic and polycarbonate backing only, have not been considered here. Table 1 lists the tested transparent ceramic materials and some typical values of mechanical and physical properties. The sintered Al_2O_3 and the Spinel were manufactured by the Fraunhofer Institute for Ceramic Technologies and Systems (IKTS), Dresden. The properties of these two materials and the sapphire were determined at IKTS. The AlON data have been adopted from the datasheet of Surmet Corporation, the manufacturer of this material.

The complete series of tests was conducted using one type of armour piercing (AP) projectile with steel core of calibre 7.62 mm × 51 and a total mass of 9.5 g. The steel cores had a mass of 3.7 g and a length of 23.5 mm. The impact velocity was kept constant at nominally 850 ± 15 m/s.

3. Test results and discussion

The first material tested was a high-purity, fully dense sintered α-Al_2O_3 of sub-μm grain size, manufactured by IKTS. Targets were assembled with ceramic front layers of 1.3 mm, 1.5 mm, 2 mm and 4 mm thickness. For each ceramic layer thickness the minimum glass backing thickness was determined, where the projectile could be stopped. In all tests yaw and pitch of the projectiles were measured by means of flash radiographs. The residual velocities of the projectiles were determined from double exposure flash radiographs. Fig. 2 gives an example of flash X-ray pictures of a test where the projectile was stopped (top) and of a case with perforation of the target (bottom). The film was exposed three times in both cases. The first exposure shows the projectile shortly before impact, whereas the second and third exposures visualize the target deformation and the residual projectile at two different times after perforation, respectively.

Fig. 3 shows the residual velocity of the projectiles as a function of the total areal density of the targets. The total areal density ρ_{FTOT} is the sum of the areal densities of the three target components, whereas the areal density of the components is defined as the product of the material density and the thickness, respectively. Consider for example the targets with a 1.5 mm Al_2O_3 front layer and a total areal density of ∼85 kg/m^2. These targets were assembled from 1.5 mm Al_2O_3,

Table 1
Properties of transparent ceramics

Material	Young's modulus (GPa)	Hardness HV10 (GPa)	Four-point bend strength (MPa)
Sapphire	~400	15–16	400–600
Sintered Al_2O_3	~400	20.5–21.5	600–700
Sintered $MgAl_2O_4$ Spinel	~275	14.5–15	200–250
AlON	323	1850 MPa Knoop Ind. 200 g	–

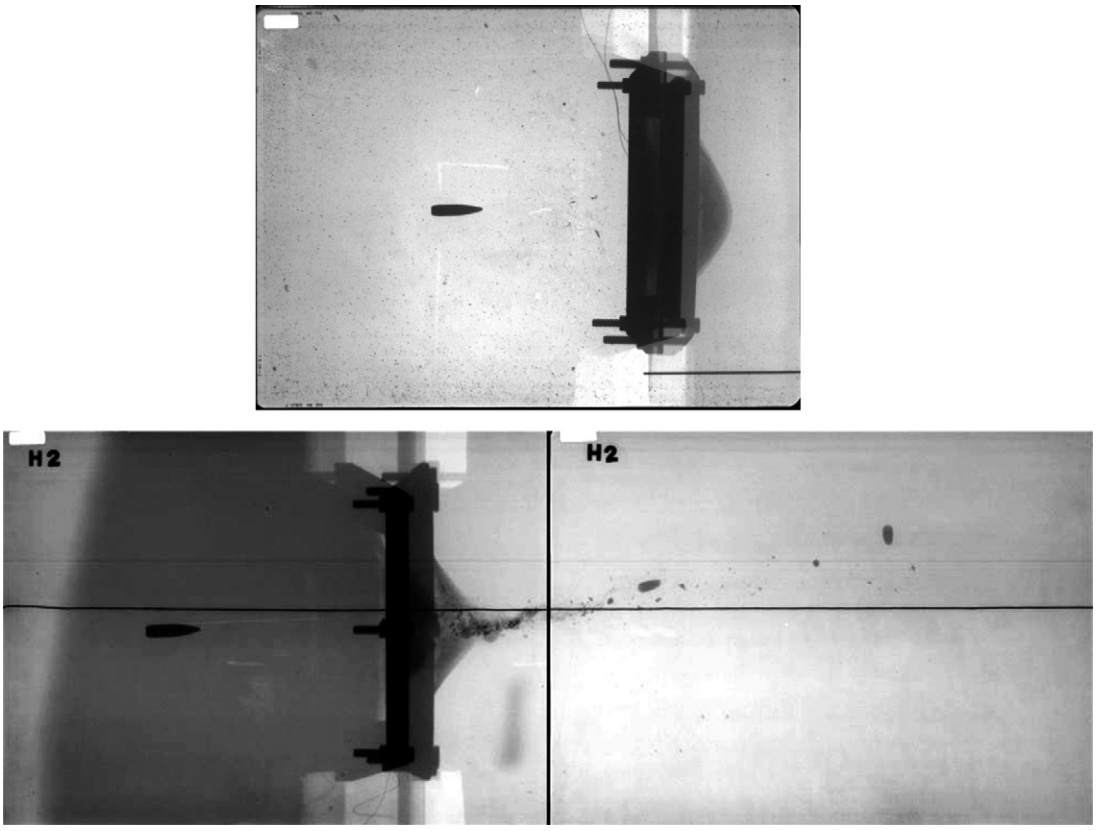

Fig. 2. Flash X-ray pictures of projectile defeat (top) and perforation (bottom) by Al_2O_3/glass/polycarbonate targets.

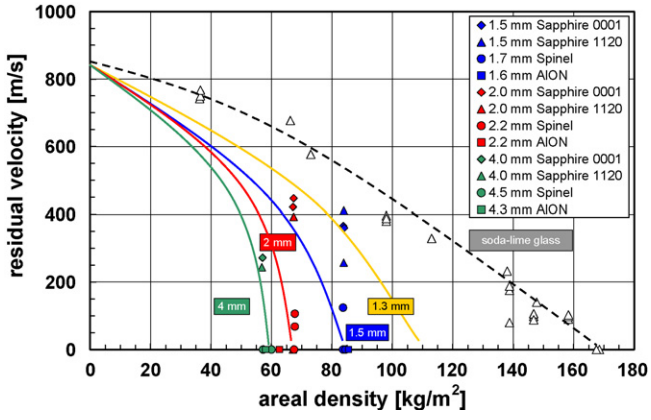

Fig. 3. Residual velocity versus areal density for ceramic/glass/polycarbonate targets.

$2 \times 15\,\text{mm} = 15\,\text{mm} + 15\,\text{mm}$ glass and 4 mm polycarbonate:

$$\rho_{\text{FTOT}} = 1.5\,\text{mm} \times 3.99\,\text{g/cm}^3 + 30\,\text{mm} \times 2.5\,\text{g/cm}^3 + 4\,\text{mm} \times 1.18\,\text{g/cm}^3 = 85.7\,\text{kg/m}^2$$

The open triangles along with the dashed black line represent the results with soda-lime glass/polycarbonate targets. These results are used as a reference or baseline for comparison with the results of the ceramic/glass/polycarbonate targets. The solid coloured lines represent the results with sintered Al_2O_3 front layers of different thickness. The values of the ballistic limit areal densities (i.e. residual velocity = zero) for the different sintered Al_2O_3 front layer thicknesses are based on three tests where the projectile was stopped, respectively. The solid lines are depicted as guidelines, but do not represent best-fit curves of the experimental data. Each colour stands for one ceramic layer thickness with all materials. The materials are distinguished by the symbols. For the sake of clarity the symbols are omitted with the sintered Al_2O_3.

The curves of the sintered Al_2O_3 clearly demonstrate that even with a thin ceramic front layer significant weight savings can be achieved compared to the reference glass/polymer system. The ballistic performance increases as the thickness T_{Cer} of the ceramic front layer increases up to $T_{Cer} = 4$ mm. Several tests have been performed (data not shown in Fig. 3) with opaque sintered Al_2O_3 surrogate material and transparent Spinel and AlON front layers of 6 mm and 8 mm thickness. The minimum areal density, sufficient to stop the projectile, which could be achieved with those targets, was also ≈60 kg/m^2. Thus, no significant increase of efficiency against the test projectile was observed with ceramic front layers of more than 4 mm thickness.

Sapphire specimens of two different crystal orientations (0001 and 1120) were tested. It can be recognized from the data in Fig. 3, that with a Sapphire thickness of 1.5 mm and 2 mm residual velocities of about 400 m/s were observed with target set-ups, which stopped the projectile when sintered Al_2O_3 was used as front layer. Residual velocities of ∼250 m/s occurred with Sapphire specimens of 4 mm thickness. No significant difference of the ballistic resistance was observed between both crystal orientations.

With the Spinel not only perforation but also projectile defeat was observed at ceramic thickness of 1.7 mm and 2.2 mm. The maximum residual velocities were ∼120 m/s. No perforation occurred at 4 mm Spinel thickness. This means, the protective strength of the tested Spinel was nearly as good as that of the sintered Al_2O_3, and significantly higher than that of Sapphire.

With AlON two tests were performed with ceramic thickness of 1.6 mm, 2.2 mm and 4.3 mm, respectively. No perforation of the targets was observed in these tests.

The efficiency of the ceramic/glass/polycarbonate targets and the possible weight savings are illustrated in Fig. 4, which shows the areal density of targets which stop the projectile, with front layers of the different tested transparent ceramics. Fig. 4 clearly demonstrates, that already a thin ceramic front layer of about 2 mm thickness allows for weight savings of more than 50% against the type of projectile considered. Whereas sintered Al_2O_3, Spinel and AlON exhibit a similar ballistic performance, a lower ballistic resistance was observed with sapphire front layers. However, Sapphire front layers also enabled significant weight savings compared to conventional transparent armour.

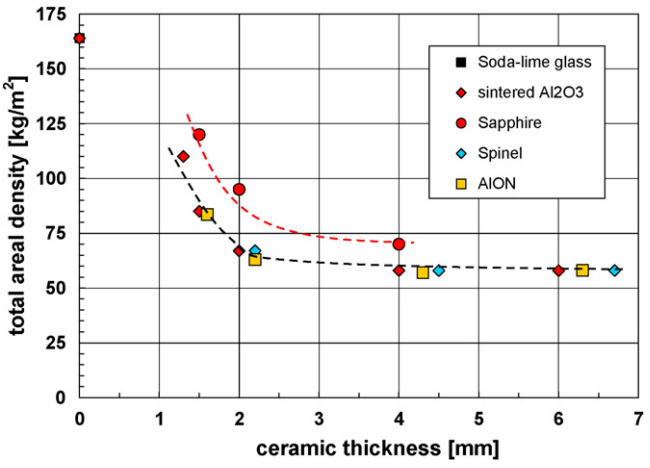

Fig. 4. Areal density versus ceramic front layer thickness for different transparent ceramics.

In order to understand the ballistic resistance of the different ceramics it is on one hand necessary to know the influence of the microstructure and the mechanical and physical properties. On the other hand, it is important to know the course of events in the interaction of the projectile and the target. Since the pioneering studies of Wilkins,[6] who examined the interaction of 7.62 mm AP projectiles with thin ceramic/aluminium targets, it is known, that penetration of the ceramic is preceded by a so-called dwell-phase of a duration of ∼10–20 μs, during which the projectile does almost not penetrate the ceramic, but is being eroded. Several studies with small calibre projectiles on the dwell phenomenon[7,8] have demonstrated that erosion or "wear" of the steel core is one key factor in the energy dissipation of the projectile and thus, for the ballistic resistance. Other key factors are Young's modulus (especially during the dwell phase), the mode of fragmentation (influenced by the microstructure, stiffness of the backing and confinement) and the hardness. Based on the ballistic results and the studies of Krell[9] on the influences on ceramic wear, Krell and Strassburger postulated a hierarchy of key influences on the protective strength of ceramic armour.[10] The importance of the contributions of the key factors will be different, depending on the projectile–target interaction during the dwell and penetration phase, determined by the specific projectile–target configuration.

4. Flash X-ray cinematography of transparent armour

In order to verify the hypothesis of the hierarchy of influences on the protective strength of ceramics two types of experiments are needed, which allow on one hand to determine the mode of fragmentation for different materials and target designs, and on the other hand to determine the duration of the dwell and penetration phase. At EMI a novel flash X-ray imaging method has been developed,[11,12] which is especially useful for the observation of the different projectile–target interaction phases. A schematic of the measurement set-up for flash X-ray cinematography is shown in Fig. 5. Instead of several separate X-ray tubes one multi-anode tube is utilized. In the multi-anode tube eight anodes are arranged on a circle of ≈12 cm diameter. This configuration causes only a relatively small parallax for the projections from the different anodes. The process under observation can be X-rayed at eight different times. The radiation transmitted through the target is then detected on a fluorescent screen. The position of the target is between the multi-anode tube and the fluorescent screen, relatively close to the fluorescent screen. The fluorescent screen converts the radiograph into an image in the visible wavelength range, which is photographed by means of an intensified digital high-speed camera. The maximum frame rate that can be achieved with such a system depends on the decay time of the fluorescent screen, the time characteristics of the intensifier and the camera. Frame rates of 100,000 fps have been achieved with a fast decaying fluorescent screen and have been used in this study.

A typical target set-up for flash X-ray cinematography is depicted in Fig. 6. The transparent ceramic specimen had a

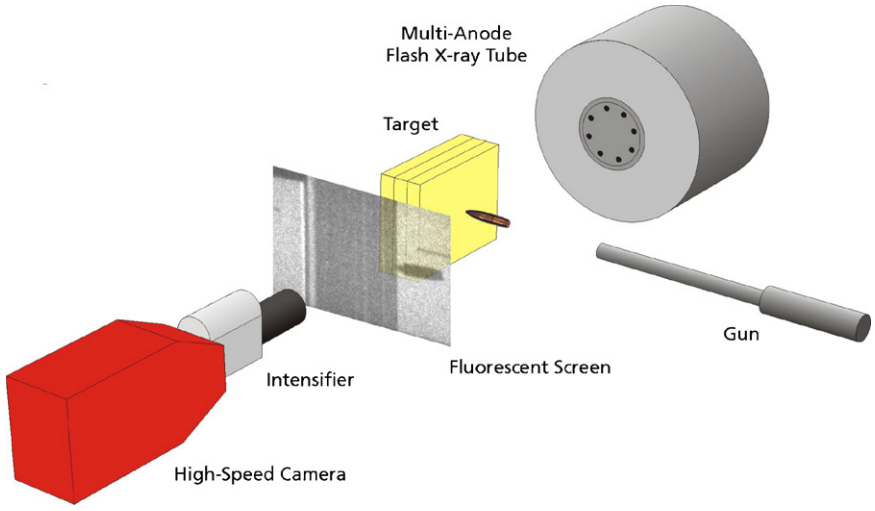

Fig. 5. Schematic of typical flash X-ray cinematography set-up.

typical size of 30 mm × 30 mm. The dimensions of the glass layers were 75 mm × 35 mm. The target dimensions were chosen such, that the transmission of X-rays through the target was sufficiently high in order to get images with a good contrast.

Fig. 7 illustrates the penetration of a 7.62 mm AP projectile into a glass/polymer laminate, consisting of six glass layers and a polycarbonate layer at the back. The eight flash radiographs from one test clearly demonstrate, that the steel core of the projectile stayed intact during penetration, which limits the efficiency of conventional transparent armor without a ceramic front.

A second test was conducted with an equal target configuration and impact conditions, where the times of the flash X-rays were shifted by 5 μs compared to the first test. The positions of the projectile nose in relation to the target surface were measured. The penetration curve, determined from both tests, is depicted in Fig. 8, which shows the position of the projectile nose as a function of time. The impact velocity was 850 m/s. The slope of the position–time curve yields a penetration velocity of 790 m/s at 10 μs after impact, which continuously decreases to

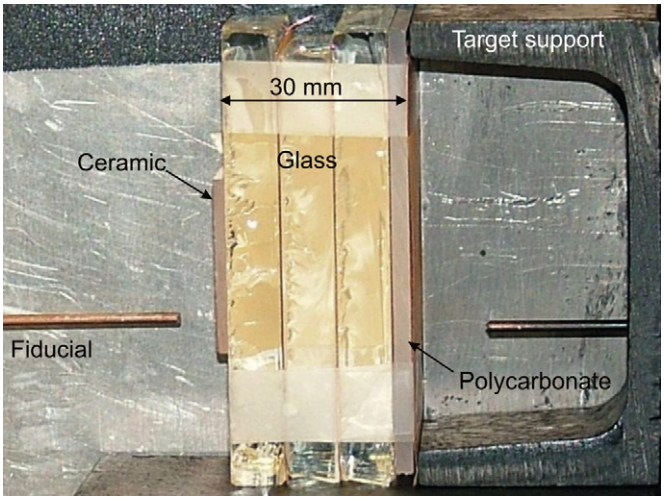

Fig. 6. Photograph of typical target set-up for flash X-ray cinematography.

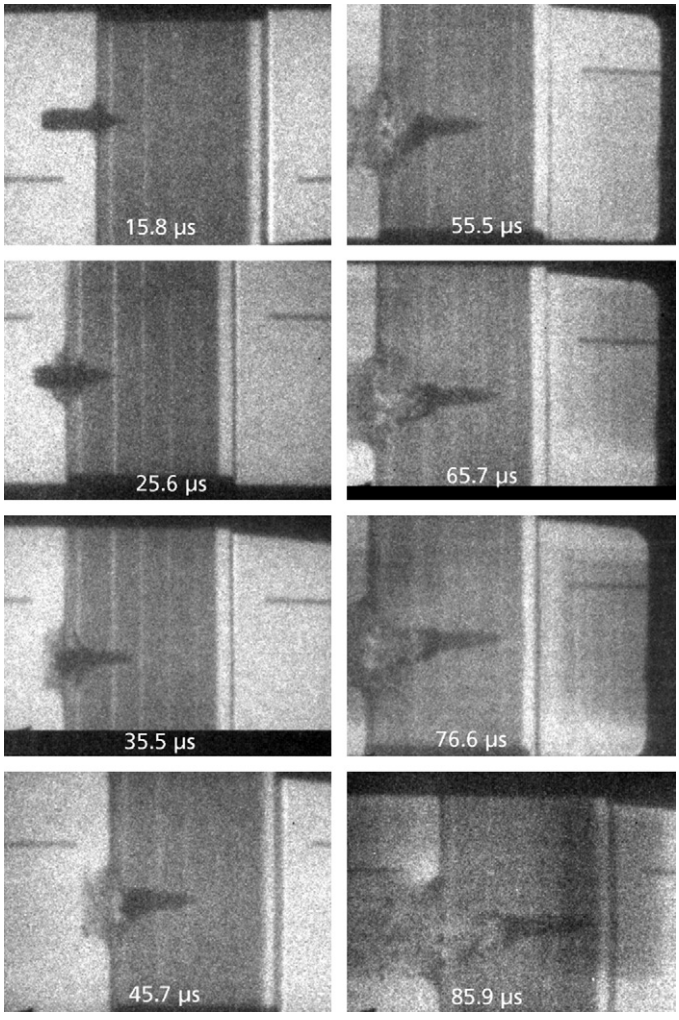

Fig. 7. Flash X-ray cinematography of 7.62 mm AP projectile penetrating a glass/polymer laminate.

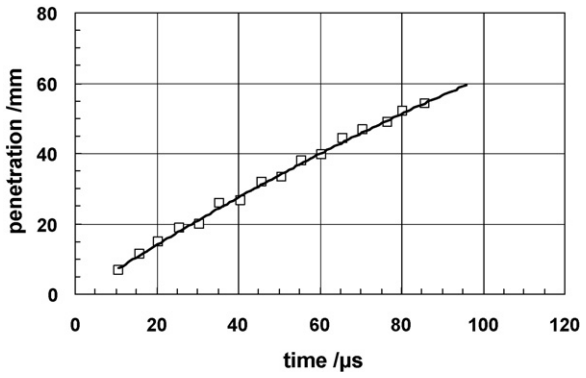

Fig. 8. Penetration into a glass–laminate: projectile nose position versus time.

about 530 m/s at 80 µs. In these two tests the projectile perforated the target.

A very different penetration process can be observed with a ceramic front layer. Fig. 9 illustrates the penetration of a 7.62 mm AP projectile into a ceramic/glass/polycarbonate target, consisting of 4 mm sub-µm grain size sintered Al_2O_3, $3 \times 9\,mm = 9\,mm + 9\,mm + 9\,mm$ borosilicate glass and 3 mm polycarbonate.

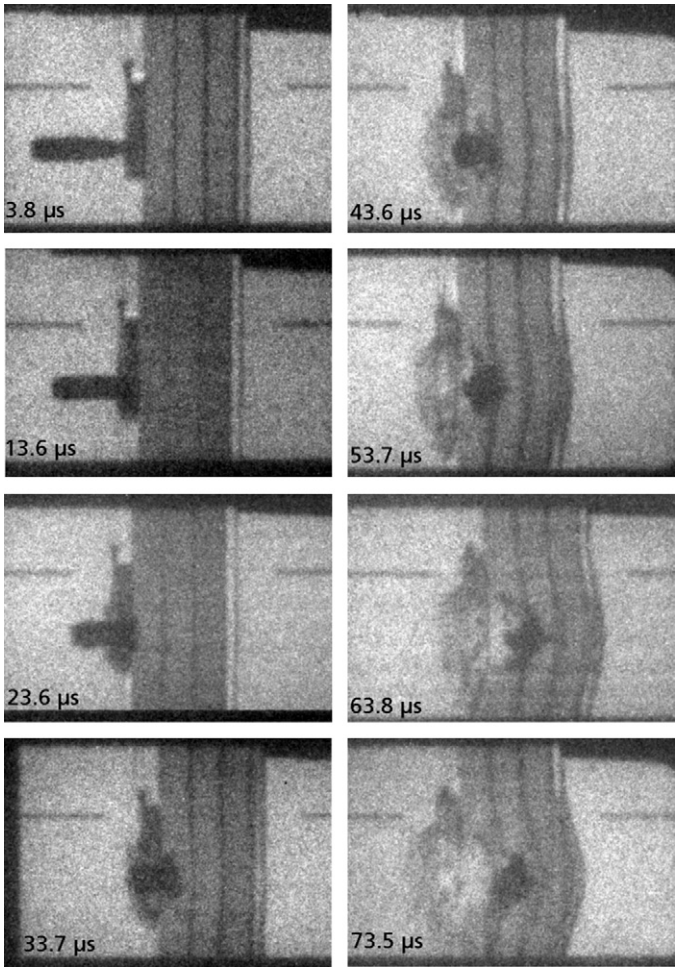

Fig. 9. Flash X-ray cinematography of 7.62 mm AP projectile penetrating a ceramic/glass/polymer laminate.

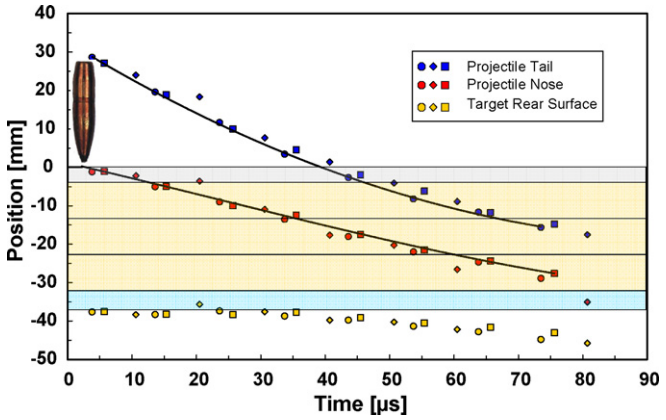

Fig. 10. Position–time histories of projectile tail, nose and target rear surface.

The projectile did not penetrate the first glass layer until 23 µs after impact. During the interaction with the ceramic front layer the length of the projectile was significantly reduced by erosion. The strong effect of the ceramic layer on the projectile is remarkable, particularly with regard to the small size (30 mm × 30 mm) and thickness of the ceramic tile and the fact, that it was hit off centre. In order to visualize the interfaces between the single glass layers, thin copper foils were inserted between the glass layers. Due to the higher X-ray absorption in the copper the interfaces appear dark.

Three tests were performed with equal ceramic/glass/polycarbonate configurations and impact conditions. The times of the X-ray flashes were shifted from test to test: in the first test the flash times were set to 3, 13, 23, . . ., 63, 73 µs (see Fig. 9). In the second test the flash times were 5, 15, . . ., 75 µs and 10, 20, . . ., 80 µs in the third test. The position–time histories of the projectile tail, nose and the target rear surface are shown in Fig. 10. The results from the different tests are represented by different symbols in Fig. 10, whereas the tail, nose and target rear surface positions are distinguished by different colours. The surface of the ceramic front layer is at the zero position on the ordinate. The path-time histories indicate, that only little penetration occurred during the first 10 µs. After this dwell phase a penetration velocity of about 400 m/s was observed. During the time interval of observation the penetration velocity decreased to about 220 m/s. The projectile was stopped with this target configuration.

About 40 µs after impact a strong deformation of the glass layers seems to begin. It is obvious, that a brittle material like glass cannot support such deformations without failure. Since the density changes in the material associated with crack formation are too small and the resolution of the X-ray imaging system is not sufficient, failure cannot be visualized with this technique. However, failure and damage evolution in transparent armour can be visualized by means of high-speed photographic methods.

5. Conclusions

High weight reductions in comparison to conventional transparent armour, which consists typically of

glass–plastics–laminates, can be achieved by the use of a hard front layer of transparent ceramic. A target set-up has been developed which allows discriminating between the ballistic performances of ceramic used as striking ply for transparent amour. The protective strength of four different transparent ceramics has been assessed by ballistic tests, using armour piercing projectiles with steel core and ceramic–glass–polycarbonate targets. The main results of the ballistic tests are summarized in the following:

- The protective strength and the efficiency of the ceramic/glass/polycarbonate targets increases as the ceramic thickness increases up to a ceramic thickness of 4 mm.
- The strongest increase in efficiency is observed in the thickness range from 1 to 2 mm.
- The increase in efficiency is related to the onset and increase of erosion of the steel core of the projectiles.
- Weight savings of about 50% could already be achieved with a ceramic front layer of 1.5 mm thickness.
- No significant increase in efficiency with increasing ceramic thickness has been observed for targets with ceramic front layers in the thickness range from 4 to 8 mm.
- Targets with a front layer of sintered Al_2O_3 exhibited the highest protective strength, followed by targets with AlON, Spinel and Sapphire.
- A novel flash X-ray imaging method has been applied to transparent armour, which allows to visualize the penetration of the projectile, and therefore, to determine the duration of different penetration phases.
- The combination of the presented ballistic testing method and visualization techniques provides a basis for a systematic optimization of transparent armour.

References

1. Ballard, C. P. Jr., *Transparent ceramic armor*. Sandia Laboratories Report SAND77-1736, 1978.
2. Patel, J and Gilde, G. A., Transparent armor materials: needs and requirements. Ceramic transactions. In *Proceedings of the Ceramic Armor Materials by Design Symposium, vol. 134*, 2001, pp. 573–586.
3. Patterson, M. C. L., Roy, D. W. and Gilde, G., An investigation of the transmission properties and ballistic performance of hot pressed spinel. Ceramic transactions. In *Proceedings of the Ceramic Armor Materials by Design Symposium, vol. 134*, 2001, pp. 595–608.
4. Krell, A. and Strassburger, E., High-purity submicron α-Al_2O_3 armor ceramics: design, manufacture and ballistic performance. Ceramic transactions. In *Proceedings of the Ceramic Armor Materials by Design Symposium, vol. 134*, 2001, pp. 463–471.
5. Krell, A., Hutzler, T. and Klimke, J., Transparent ceramics: transmission physics and consequences for materials selection, manufacturing and applications, *J. Eur. Ceram. Soc.* [this volume].
6. Wilkins, M. L., *Third progress report on Light Armor Program*. UCRL-50460, Lawrence Livermore Laboratory, Livermore, CA, USA, 1968.
7. Gooch, W. A., Burkins, M. S., Kingman, P., Hauver, G., Netherwood, P. and Benck, R., Dynamic X-ray imaging of 7.62-mm APM2 projectiles penetrating boron carbide. In *Proceedings of the 18th International Symposium on Ballistics, vol. 2*, 1999, pp. 901–908.
8. Anderson Jr., C. E., Burkins, M. S., Walker, J. D. and Gooch, W. A., Time-resolved penetration of B_4C tiles by the APM2 bullet. *Comp. Model. Eng. Sci.*, 2005, **8**, 91–104, No. 2.
9. Krell, A., Improved hardness hierarchic influences on wear in submicron sintered alumina. *Mater. Sci. Eng. A*, 1996, **209**(1–2), 156–163.
10. Krell, A. and Strassburger, E., Hierarchy of key influences on the ballistic strength of opaque and transparent armor. *Am. Ceram. Soc. Bull.*, 2007, **86**(4).
11. Helberg, P., Nau, S. and Thoma, K., High-speed Flash X-ray Cinematography. In *Ninth European Conference for Nondestructive Testing*, September 2006.
12. Thoma, K., Helberg, P. and Strassburger, E., Real time-resolved flash X-ray cinematographic investigation of interface defeat and numerical simulation validation. In *Proceedings of the 23rd International Symposium on Ballistics, vol. 2*, 2007, pp. 1065–1072.